Special Feature: Nano Structured Devices

Research Report

Silicon Resonator Applied to Flat Ultra-thin Grating Lenses

Takayuki Matsui, Shuichi Yamashita, Hiroyuki Wado and Hideo Iizuka

Report received on Jul. 15, 2019

ABSTRACT Silicon metasurface structures that exhibit perfect absorption and focusing ability are presented. High refractive index silicon enables light confinement in the silicon nanoblocks, and tunability of the coupling rate is provided via the nanoblock geometric parameter. Unity absorption of the structure becomes possible when the coupling rate of the reflection resonance structure to the reflection port is identical to the internal loss rate. Such an absorption characteristic is derived from the general resonance model; therefore, the structure has the flexibility of the functional lossy layer position, even when the layer is apart from the nanoblock resonator. A flat silicon metasurface lens comprising 2D unit cells was experimentally demonstrated. A gradual change of the filling factor of the nanoblocks in the unit cell around sharp resonance enables balancing high transmittance and a phase coverage of 0–2π. The focused profiles of the fabricated lenses were in good agreement with the calculation results, and a numerical aperture of up to 0.707 was confirmed.

KEYWORDS Metasurface, Grating, Perfect Absorption, Resonator, Optics, Metamaterial

1. Introduction

Exploring light-matter interaction is fundamentally and industrially important to effectively utilize a coherent or an incoherent light source in limited spaces for integrated optics.(1-5) Maximization of the interaction can significantly reduce material usage and can alter the expensive material to inexpensive one. Light confinement in a small space is one of the promising applications of light-matter interaction. Due to the uncertainty, spatial light confinement in small spaces can be inversely proportional to the spread of the magnitude of wavevector,(1) $\Delta x \geq {}^{1}/_{2\Delta k_x}$.

When the variance of the magnitude of the wavevector is larger, the spatial confinement is smaller. The practical limit in a free space or homogeneous dielectric media using conventional optics is expressed as $\Delta_{r_s} = 0.61\,{}^{\lambda}/_{NA}$, where λ is the wavelength in a vacuum and NA is the numerical aperture of the optics. In the case that conventional free space optics are used, the practical limit of NA is around 1.4. Therefore, the spatial confinement is around half the wavelength. Improvements in nanofabrication processes, facilities, and computer-aided design (CAD)-based simulation techniques have meant that structures with dimensions less than the wavelength have become accessible for researchers and developers. Such recent technologies have extended the conventional research field of light-matter interaction using artificial structures known as metamaterials/metasurfaces.

In view of light confinement in small spaces, the metamaterial/metasurface research community mainly uses metal or high refractive index dielectrics as building materials. The research field that uses the former is known as plasmonics,(6-8) while the latter is used in the field of metasurfaces.(9,10)

In this review, we present our recent advances in metasurfaces using silicon as a high-refractive index material.(11,12) Silicon nanostructures efficiently capture the incident light over more than its cross-sectional area, which maximizes enhancement of the interaction for phase manipulation and absorption. We will start from the general resonance model to explain the role of the silicon nanostructure, and then introduce recent progress in our research, that is, the development of a perfect absorption structure and a flat metasurface lens. Both research fields have been extensively investigated in recent decades,(13-21) which has contributed to the extension of these fields to optoelectronics applications.

2. General Resonator Model

Coupling of a resonator system is a promising way to increase light-matter interaction; therefore, we start by considering a general two-port system comprised of a resonator with a resonant frequency of ω_0 and an intrinsic damping rate of γ_0 in the region of $\omega_0 \gg \gamma_0$, as shown in **Fig. 1**(a). The resonator is coupled to Ports 1 and 2 with coupling rates of $\sqrt{2\gamma_1}$ and $\sqrt{2\gamma_2}$, respectively, where γ_1 and γ_2 represent the mode decay of the resonator due to the power escaping from each of the two ports. S_{1+}, S_{2-}, and S_{1-} are respectively the input, transmissive, and reflective wave amplitudes and there is no power input in Port 2, $S_{2+} = 0$. The transmittance, reflectance, and absorbance are given by the coupled mode theory:(2,22)

$$T = \left| {S_{2-}}/{S_{1+}} \right|^2 = \frac{4\gamma_1\gamma_2}{(\omega-\omega_0)^2+(\gamma_0+\gamma_1+\gamma_2)^2}, \quad (1)$$

$$R = \left| {S_{1-}}/{S_{1+}} \right|^2 = \frac{(\omega-\omega_0)^2+(\gamma_0-\gamma_1+\gamma_2)^2}{(\omega-\omega_0)^2+(\gamma_0+\gamma_1+\gamma_2)^2}, \quad (2)$$

$$A = 1 - R - T = \frac{4\gamma_0\gamma_1}{(\omega-\omega_0)^2+(\gamma_0+\gamma_1+\gamma_2)^2}. \quad (3)$$

In Eqs. (1)-(3), unity (i) transmission, (ii) reflection, and (iii) absorption are obtained at $\omega = \omega_0$ when the following conditions are fulfilled: (i) $\gamma_1 = \gamma_2$ *and* $\gamma_0 \sim 0$, (ii) $\gamma_2 \sim 0$ *and* $\gamma_0 \sim 0$, and (iii) $\gamma_0 = \gamma_1$ *and* $\gamma_2 \sim 0$, respectively. Figure 1(b) shows calculated plots with parameter sets of $\gamma_0 = \gamma_1$ with $\gamma_0 = 0.001\omega_0$ for unity absorption. Here we pursue the unity absorption case in detail; the parameters claim the absorption rate of a mode in the resonator is equal to the leakage rate of the mode to Port 1, and the resonator is critically coupled to Port 1 without coupling to Port 2, and all incident light is absorbed. Once the absorption rate of resonator is determined from the material selection, a spectral shape similar to the full width at half maximum (FWHM) can be expected for a two-port system. Thus, a perfect absorption structure that is tailored for the material properties is possible, and a broadband, highly transmissive structure with phase modulation is also possible.

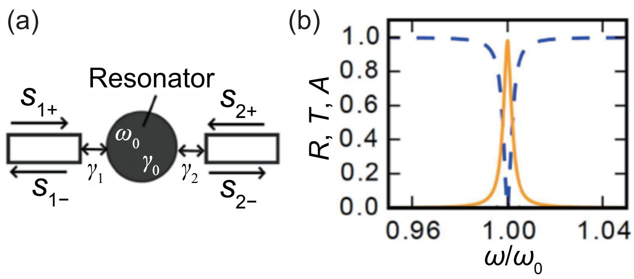

Fig. 1 (a) Analytical model for a two-port system consisting of a resonator. (b) Transmittance (black dotted line), reflectance (blue dashed line), and absorbance (orange solid line) for the analytical model with $\gamma_0 = \gamma_1 = 0.001\omega_0$ and $\gamma_2 = 0.02\gamma_0$. Transmittance is less than 0.02.

3. Unity Absorption in Ultra-thin Lossy Layer on Transparent Substrate

In the previous section, a unity absorption condition is claimed, where a reflection resonator system with the leakage rate to Port 1 being equal to the absorption rate of the selected material is indispensable. Equations (1)-(3) are based on the general resonance model (Fig. 1) and are therefore not limited by the geometry. We have previously presented a unity absorption structure using vanadium dioxide (VO_2) that exhibits a phase transition between the insulating and metallic states around 340 K, which has contributed to the realization of various functional devices. Silicon nanoblocks are selected for the metasurface structure, along with a VO_2 absorption layer and a sapphire substrate in the structure (**Figs. 2**(a) and (b)). A 26 nm VO_2 layer is added to the reflection resonance structure, and the spectrum is shown in Fig. 2(d). A near-unity absorbance of 0.98 is obtained around 1550 nm, which is approximately 25 times larger than the case without a nanoblock resonator (0.04).

Equations (1)-(3) represent only a general model, and the nanoblocks do not necessarily touch the absorption layer in our structure, as long as the structure is electromagnetically coupled to the absorption layer, i.e., as long as the evanescently decaying electromagnetic field from the high-refractive-index resonator reaches the absorption layer. This feature expands the flexibility for practical designs, e.g., a coating film can be inserted between the VO_2 film and the nanoblocks (Fig. 2(e)). The absorption spectra of the structure are calculated with variation of the thickness of the coating between the VO_2

layer and the nanoblock t_{gap} , and the spectral curves are plotted in Fig. 2(f). The use of sapphire for the coating is assumed. High absorption is obtained when t_{gap} = 300 nm, which decreases as the coating becomes thicker. It is noteworthy that this structure provides unity absorption and has flexibility of the placement of the absorption layer with respect to the nanoblocks.

4. Flat Metasurface Lenses

In the previous section, a unity absorption structure is presented; the resonance conditions where $\gamma_0 = \gamma_1 \; and \; \gamma_2 \approx 0$ are fulfilled. In this section, we would like to present another advancement of this research, which is a flat transmission metasurface lens that uses the reflection resonance condition of $\gamma_2 \approx 0 \; and \; \gamma_0 \approx 0$. Silicon nanoblocks can confine light in the nanoblocks, and the transmission phase becomes sensitive to changes in the geometric shape. Silicon is known to be transparent around the near-infrared range; therefore, intrinsic absorption loss is negligibly small in this wavelength range. Given that the nanoblocks are appropriately designed with a sharp FWHM spectrum, then the transmission around the reflection resonance is quite high with a widely variable transmission phase, as shown in **Figs. 3**. Combining this resonance-related transmission with the effective index change gives rise to an ideal transmission phase control with high transmittance, which is the basic concept of the proposed metasurface lens.

The lens discussed in this study comprises a square array of square ridges, in which each unit cell has the same pitch but different ridge widths, as shown in Figs. 3(a)-(c). Ridge widths were determined to set

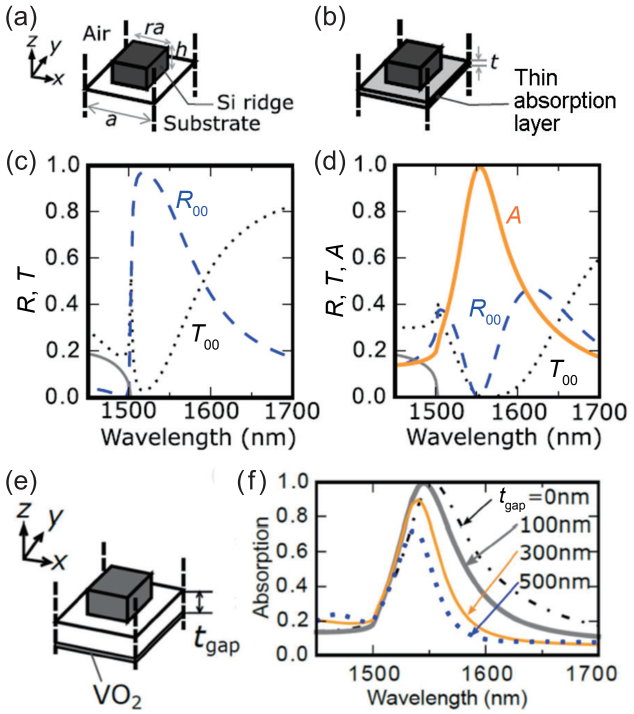

Fig. 2 (a) Resonant structure configuration. (b) Configuration of a resonant structure with a thin absorption layer. (c)(d) Calculated spectra, where A, R_{00}, and T_{00} denote the absorbance, reflectance, and transmittance, and the subscripts refer to the diffraction orders in the x and y directions. (e) Configuration of a resonant structure that is electromagnetically coupled to the absorption layer. (f) Absorbance spectra with coating thicknesses (t_{gap}) of 0 nm (black dash-dotted line), 100 nm (gray thick solid line), 300 nm (orange solid line), and 500 nm (blue dotted line).

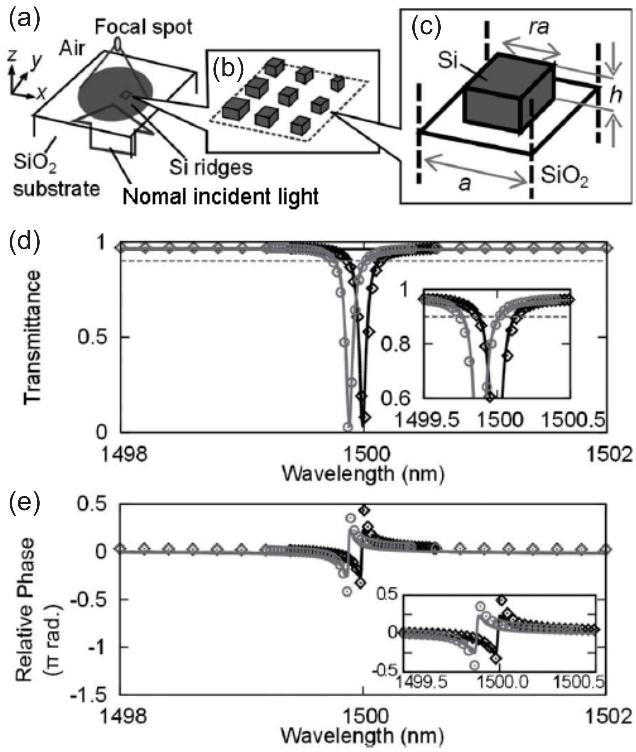

Fig. 3 (a) Schematic diagram of a grating lens. (b) Magnified view of the grating lens. Each nanoblock size is gradually changed from the center to the circumference in the lens. (c) Unit cell structure considered in this study. (d) Transmittance and (e) relative transmission phase. Symbols and lines represent numerical results obtained by numerical calculation plots and analytical results based on Eq. (1).

a designed phase profile ϕ, for the lens. A hyperbolic phase profile for the lens is geometrically determined, and is expressed as $\phi(x,y) = \frac{2\pi}{\lambda}\left(\sqrt{x^2+y^2+f^2}-f\right)$ where f is the focal length, and λ is the wavelength in a vacuum. The unit cell design of the silicon ridge must have phase coverage of 0–2π to achieve any focal lengths with the lens. The transmission coefficients of the unit cell were calculated by varying the pitch and the fill factor with a fixed height of 1100 nm, and the zeroth-order transmittance and the relative phase in **Figs. 4**(a) and (b), respectively. The transmission dip from a = 600 nm with r = 0.6 to a = 1000 nm with r = 0.32 in Fig. 4(a) corresponds to the reflection resonance of the unit cell, and this resonance was only exhibited under a narrow fill factor condition at around a = 800 nm. The insets in Figs. 4(a) and (b) are line graphs of the transmittance and transmission phase at a = 800 nm. High transmittance (> 90%) and phase coverage of 0–2π can be obtained in the fill factor range of 0.2–0.5; therefore, a pitch of 800 nm was adopted for the grating lens.

Four grating lenses with aperture diameters of 150 μm were experimentally tested, where the focal lengths were f = 300λ_0, 200λ_0, 100λ_0, and 50λ_0. **Figure 5**(a) shows scanning electron microscopy (SEM) images of the fabricated structure. The lenses were experimentally evaluated using a custom built near-infrared microscope system. A linearly x-polarized laser at λ = 1500 nm was irradiated from the substrate side, and focused to a spot in the air region after passing through the lens. The focused intensity profile

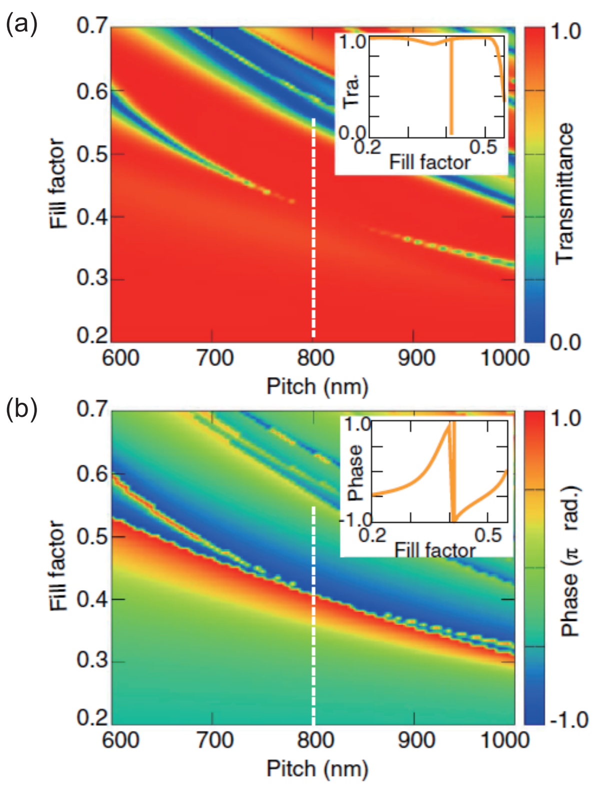

Fig. 4 Numerically calculated zeroth order (a) transmittance and (b) transmission-phase distributions of the unit cell. Insets represent line graphs at 800 nm, which correspond to the white dashed lines in the figures.

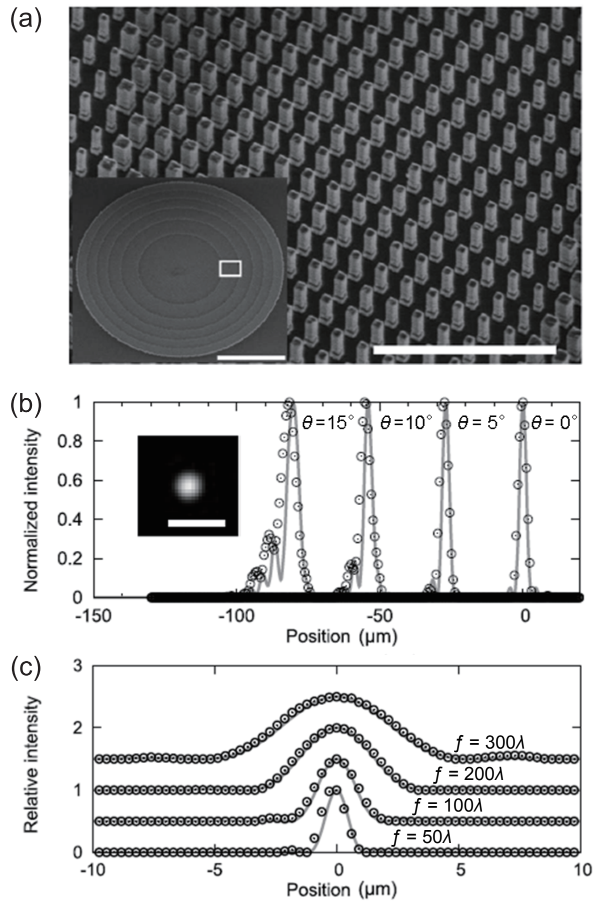

Fig. 5 (a) SEM image of the fabricated lens. The inset shows an entire view of the lens. Scale bars are 50 μm for the inset and 5 μm for the main image. (b) Intensity profiles through the fabricated grating lens with various incident angles. The inset shows a focal image with θ = 0°. The scale bar is 10 μm. Magnification (M) and numerical aperture (NA) of the objective lens were 50 × and 0.55, respectively. (c) Intensity profiles through the lenses with various focal lengths. An objective lens with M = 100 × and NA = 0.85 was used for measurements.

was recorded on a near-infrared camera through the microscope. The lens pattern was invariant to both directions (x and y) due to the geometric symmetry; therefore, one-directional intensity profiles (x-direction) were mainly evaluated.

Intensity profiles of the lens with various incident angles of θ = 0°, 5°, 10°, and 15° are shown in Fig. 5(a), and an intensity image with θ = 0° on the camera is shown as an inset. To evaluate the fabricated lenses accurately, experimental intensity profiles were compared with the diffraction integral formula. Figure 5(b) shows the intensity profiles with various focal lengths at each focal plane. The intensity profiles are also in good agreement with the calculated lines, and numerical aperture (*NA*) values from 0.164 to 0.707 were experimentally validated.

5. Summary

Our recent advances in the field of flat metasurface research are presented. A concept was introduced whereby unity absorption and transmission phase control were achieved via a general resonance model. We have explored the absorption behavior of an ultra-thin lossy layer attached to a transparent dielectric substrate that is electromagnetically coupled to a high-refractive-index transparent resonant structure consisting of nanoblocks. The structure provided unity absorption and has flexibility of the absorption layer placement with respect to the nanoblocks. The performance of the structure is not limited by the materials as long as the condition for excitation of the resonance is fulfilled.

A flat dielectric grating lens comprising 2D unit cells was experimentally demonstrated. Selection of the geometric parameter of the unit cell around a sharp resonance condition results in a balanced high transmittance and phase coverage of 0–2π. Focused profiles of the fabricated lenses were in good agreement with the calculation results. Based on the concept of a transmissive lens in this study, we consider that the proposed lens could be integrated into infrared sensor systems.

References

(1) Novotny, L. and Hecht, B., *Principles of Nano-Optics* (2012), 564p., Cambridge University Press.

(2) Haus, H. A., *Waves and Fields in Optoelectronics* (1984), 402p., Prentice-Hall.

(3) Atwater, H. A. and Polman, A., “Plasmonics for Improved Photovoltaic Devices”, *Nature Materials*, Vol. 9 (2010), pp. 205-213.

(4) Oulton, R. F., Sorger, V. J., Zentgraf, T., Ma, R.-M., Gladden, C., Dai, L., Bartal, G. and Zhang, X., “Plasmon Lasers at Deep Subwavelength Scale”, *Nature*, Vol. 461 (2009), pp. 629-632.

(5) Kuroda, K., *Butsuri Kōgaku* (in Japanese) (2011), 210p., *Asakura Shoten*.

(6) Maier, S. A., *Plasmonics: Fundamentals and Applications* (2007), 223p., Springer.

(7) Okamoto, T. and Kajikawa, K., *Plasmonics* (in Japanese) (2010), 272p., *Kōdansha*.

(8) Kajikawa, K., Okamoto, T., Takahara, J. and Okamoto, K., *Active Plasmonics* (in Japanese) (2013), 318p., *Koronasha*.

(9) Lin, D., Fan, P., Hasman, E. and Brongersma, M. L., “Dielectric Gradient Metasurface Optical Elements”, *Science*, Vol. 345, No. 6194 (2014), pp. 298-302.

(10) Yu, N. and Capasso, F., “Flat Optics with Designer Metasurfaces”, *Nature Materials*, Vol. 13 (2014), pp. 139-150.

(11) Matsui, T., Yamashita, S., Wado, H., Fujikawa, H. and Iizuka, H., “Flat Grating Lens Utilizing Widely Variable Transmission-phase via Guided-modes”, *Optics Letters*, Vol. 40, No. 1 (2015), pp. 25-28.

(12) Matsui, T. and Iizuka, H., “Total Absorption in Ultra-thin Lossy Layer on Transparent Substrate Using Dielectric Resonance Structure”, *Journal of Optics*, Vol. 19, No.3 (2017), 03LT01.

(13) Vasudev, A. P., Schuller, J. A. and Brongersma, M. L., “Nanophotonic Light Trapping with Patterned Transparent Conductive Oxides”, *Optics Express*, Vol. 20, No. S3 (2012), pp. A385-A394.

(14) Piper, J. R. and Fan, S., “Total Absorption in a Graphene Monolayer in the Optical Regime by Critical Coupling with a Photonic Crystal Guided Resonance”, *ACS Photonics*, Vol. 1 (2014), pp. 347-353.

(15) Zhao, B., Zhao, J. M. and Zhang, Z. M., “Resonance Enhanced Absorption in a Graphene Monolayer Using Deep Metal Gratings”, *Journal of the Optical Society of America B*, Vol. 32 (2015), pp. 1176-1185.

(16) Li, W. and Valentine, J., “Metamaterial Perfect Absorber Based Hot Electron Photodetection”, *Nano Letters*, Vol. 14 (2014), pp. 3510-3514.

(17) Matsui, T., Li, Y., Hsu, M.-H. M., Merckling, C., Oulton, R. F., Cohen, L. F. and Maier, S. A., “Highly Stable Plasmon Induced Hot Hole Transfer into Silicon via a $SrTiO_3$ Passivation Interface”, *Advanced Functional Materials*, Vol. 28 (2018), 1705829.

(18) Fattal, D., Li, J., Peng, Z., Fiorentino, M. and Beausoleil, R. G., "Flat Dielectric Grating Reflectors with Focusing Abilities", *Nature Photonics*, Vol. 4 (2010), pp. 466-470.
(19) Lu, F., Sedgwick, F. G., Karagodsky, V., Chase, C. and Chang-Hasnain, C. J., "Planar High-numerical-aperture Low-loss Focusing Reflectors and Lenses Using Subwavelength High Contrast Gratings", *Optics Express*, Vol. 18 (2010), pp. 12606-12614.
(20) Khorasaninejad, M., Chen, W. T., Devlin, R. C., Oh, J., Zhu, A. Y. and Capasso, F., "Metalenses at Visible Wavelengths: Diffraction-limited Focusing and Subwavelength Resolution Imaging", *Science*, Vol. 352 (2016), pp. 1190-1194.
(21) Genevet, P., Capasso, F., Aieta, F., Khorasaninejad, M. and Devlin, R., "Recent Advances in Planar Optics: From Plasmonic to Dielectric Metasurfaces", *Optica*, Vol. 4 (2017), pp. 139-152.
(22) Joannopoulos, J. D., Johnson, S. G., Winn, J. N. and Meade, R. D., *Photonic Crystals: Molding the Flow of Light* (2008), Princeton University Press.

Takayuki Matsui
Research Field:
- Photonics
Academic Degree: Ph.D.
Academic Society:
- The Optical Society

Shuichi Yamashita*
Research Fields:
- MEMS
- Sensor
Academic Society:
- The Japan Society of Infrared Science and Technology

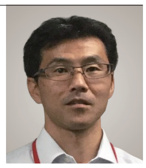

Hiroyuki Wado*
Research Fields:
- MEMS
- Sensor
Academic Degree: Ph.D.
Academic Societies:
- The Institute of Electrical Engineers of Japan
- The Japan Society of Applied Physics
Award:
- IEEJ Distinguished Paper Award, The Institute of Electrical Engineers of Japan, 2012

Hideo Iizuka
Research Field:
- Metamaterial
Academic Degree: Ph.D.
Academic Societies:
- The Optical Society
- IEEE

*DENSO CORPORATION